IMPACT LOADING OF FRPS – FROM LOW TO HIGH SPEEDS

V. V. Silberschmidt [a*], V. A. Phadnis [a], A. Roy [a]

[a]*Wolfson School of Mechanical and Manufacturing Engineering, Loughborough University, Leics., LE11 3TU, UK*
**v.silberschmidt@lboro.ac.uk*

Keywords: Carbon fibre-reinforced composites; Dynamic fracture; Finite-element analysis; Blast and ballistics

Abstract
Fibre reinforced composites (FRPs) are extensively used as protective gear where a wide range of impact loading is imposed on the components made of them. Numerical models of FRP deformation, once accurately developed, will elucidate various deformation mechanisms which drive composite failure across impact velocity envelopes. In this paper we present results obtained from air blast on FRPs and ballistics on woven composites using a numerically accurate and computationally efficient modelling framework.

1. Introduction

The ever expanding applications of composite materials expose them to severe loading and environmental conditions, posing new challenges to the designer. Fibre reinforced polymer (FRP) composites are widely used in protective structural applications due to their superior mechanical and physical properties such as durability, high strength-to-weight-ratio, and high stiffness. The range of application is wide with impact velocities (and consequently impact energies) ranging from low to high magnitudes. Such impact events need to be studied in some detail as it has been widely reported that the damage mechanisms are observed to change significantly with the nature of impact.

Rajendran and Lee [1] conducted a detailed review of the phenomena of air and underwater explosions and their effects on plane plates. They found that of the important shock wave parameters significant for an air blast, were the peak overpressure and the impulse. For an underwater explosion, the peak overpressure, time constant, free-field impulse and energy were recognised to be the four vital parameters for the damage process. Tekalur *et al*. [2] studied the effect of various fibres on the blast response of composite panels. They used two different fibre materials: E-glass and carbon, and exposed those composite panels to high strain rates and quasi-static loading. In dynamic loading, the carbon-fibre composites showed catastrophic failure, whereas E-glass-fibre composites exhibited progressive damage behaviour. Arora *et al*. [3] analysed a blast response of glass-fibre sandwich composite panels, fixed at their edges and exposed to real explosives at varying stand-off distances. They used high-speed photography and digital image correlation analysis to characterise the blast response of these panels. Damage was observed to be initiated in the form of a crack in a front

skin, giving a rise to localised delamination around the cracked region and shear cracking in the core. Interfacial failure between the front skin and the core was also observed. This study also involved a finite-element analysis to verify experimental observations such as transient boundary conditions. In ballistic impact, FRPs retard a projectile by absorbing its kinetic energy through different mechanisms such as deformation, delamination and shear between layers. The condition for perforation, also called the *ballistic limit velocity* (V_{50}) is the most important factor for design of a suitable protective structure [4]. In this regard, significant research has been carried out on the behaviour of composite materials under ballistic impact loading. Zhu *et al*. [5] investigated the response of woven Kevlar/polyester laminates of varying thicknesses to quasi-static and dynamic penetration by cylindroconical projectiles. Ballistic limits were also determined and terminal velocities measured. It was reported that deliberately introduced delamination and changes in the volume fraction of fibres did not result in significant changes in the impact resistance. Some studies revealed that a damage pattern for dynamic loading was significantly different from that in the corresponding quasi-static penetration conditions.

Numerical models for predicting the performance of woven fabric composites have been the subject of interest for many years. Most of these approaches have made an attempt to analyze composites within the framework of a 2D boundary value problem using an assumption of plane-stress or generalized plane-strain conditions [6] and hence are not effective means to analyse resulting through-thickness stress-states and underlying damage modes. Naturally, due to the complexity involved in describing the response of fabric panels to ballistic impact, most models attempt to provide the most acceptable trade-off in performance analysis. To model a woven fabric down to a level of individual yarn crossovers would certainly be preferred in order to study frictional and crimping effects, but such studies are computationally impracticable. The complexity of the problem has forced researchers to accept certain simplifying assumptions to make it computable.

The work presented here focuses on the finite-element analysis of a ballistic impact response of plain-weave E-glass fabric/epoxy composite using the general-purpose finite-element software ABAQUS/Explicit [7]. A ply-level FE model was developed, where a ply is modelled as a homogeneous orthotropic elastic material with a potential to sustain progressive stiffness degradation due to fibre/matrix cracking, and plastic deformation under shear loading. The model was implemented as a VUMAT user subroutine and was able to distinguish fibre- and matrix-related failure modes separately. Delamination was modelled using cohesive-zone elements. All FE models were validated with the experimental results and showed a reasonably good agreement

2. Finite-element model

Blast experiments are generally laborious, difficult to repeat under the same conditions and demand a plethora of safety precautions. In this regard, a validated FE model can prove to be a valuable tool to estimate the blast performance of underlying materials. Here, a dynamic FE model imitating the mechanical response of curved CFRP panels exposed to the blast was developed in commercial software ABAQUS. The details about material modelling, fluid-structure interaction, mesh and boundary conditions are discussed in the next sections.

2.1. Material Model

A user-defined 3D damage model (VUMAT) with solid elements was developed and

implemented into the finite-element code ABAQUS/EXPLICIT to predict the character and extent of damage through the laminate thickness when exposed to the blast load. Interface cohesive elements were inserted between the plies of the modelled laminate to simulate delamination. The general contact algorithm in ABAQUS/EXPLICIT was used to simulate contact conditions between the shock wave and the composite laminate, and between the layers by defining appropriate contact-pair properties. An element-deletion approach [8] was used to represent the laminate degradation based on initiation and evolution of damage in the meshed CFRP elements. The results of numerical simulations were evaluated using comparison with the experimental data.

2.2. Element deletion

The blast load induces large deformation in the FRP laminate. During the FE modelling, these excessively deformed elements can cause unreasonable increase in the simulation time or premature termination of the analysis. Hence, these elements were removed from the analysis as soon as they satisfied a stress based damage criteria based on the work of Hashin [9] and Puck [10] implemented through VUMAT in Abaqus/explicit. The details can be found in our previous work [8].

2.3 Elastic continuum-damage-mechanics model

The fibre directions of woven fabric reinforcement are assumed to be orthogonal. The constitutive stress-strain relations are formulated in a local co-ordinate system with its base vectors aligned with fibre directions. The in-plane elastic stress-strain relations are given according to orthotropic elasticity with damage [11].

$$\begin{Bmatrix} \varepsilon_{11} \\ \varepsilon_{22} \\ \varepsilon_{12}^{el} \end{Bmatrix} = \begin{pmatrix} \frac{1}{(1-d_1)E_1} & -\frac{\nu_{12}}{E_1} & 0 \\ -\frac{\nu_{21}}{E_2} & \frac{1}{(1-d_2)E_2} & 0 \\ 0 & 0 & \frac{1}{(1-d_{12})2G_{12}} \end{pmatrix} \begin{Bmatrix} \sigma_{11} \\ \sigma_{22} \\ \sigma_{12} \end{Bmatrix}, \tag{1}$$

where $\varepsilon = \left(\varepsilon_{11}, \varepsilon_{22}, \varepsilon_{12}^{el}\right)^T$ is the elastic strain vector, $\sigma = \left(\sigma_{11}, \sigma_{22}, \sigma_{12}^{el}\right)^T$ is the stress vector, E_1 and E_2 are the Young's moduli in the principal orthotropic directions; G_{12} is the in-plane shear modulus; υ_{12} and υ_{21} are the principal Poisson's ratios; d_1 and d_2 are the damage parameters associated with the fibre fracture along the principal orthotropic directions; and d_{12} is the damage parameter associated with the matrix micro-cracking due to in-plane shear deformation. The damage parameters vary between 0 and 1 and represent the stiffness degradation caused by micro-damage in the material. The material properties were obtained from [4] owing to the similarity of specimens.

2.4 Elastic-plastic shear model

The in-plane shear response is dominated by a non-linear behaviour of the matrix that exhibits both stiffness degradation due to matrix micro-cracking and plasticity [12]. The elastic part of the shear response was calculated using (1). Here, the plastic shear response of the material is considered. The matrix response may be inelastic due to extensive cracking or plasticity. This

leads to permanent deformations in the ply upon unloading. To account for these effects, a classical plasticity model with an elastic domain function and a hardening law, which is applied to the effective stresses in the damaged material, is used. The elastic domain function F is given by

$$F = \left|\tilde{\sigma}_{12}\right| - \tilde{\sigma}_0 \bar{\varepsilon}^{pl} \le 0 .$$

The hardening law obeys

$$\tilde{\sigma}_0 \bar{\varepsilon}^{pl} = \tilde{\sigma}_{y0} + C(\bar{\varepsilon}^{pl})^p$$

where $\tilde{\sigma}_{y0}$ is the initial effective shear yield stress; C and p are coefficients; and $\bar{\varepsilon}^{pl}$ is the equivalent plastic stain due to shear deformation. For the current study the following are considered: $C = 1125$; $p = 1.05$ and $\tilde{\sigma}_{y0} = 150$ MPa .

2.5 Fluid-structure coupling and shock wave loading in blast simulations

The fluid model consisted of the air inside and outside the shock tube as well as the air surrounding the plate as shown in Fig. 1. The air outside the tube was modelled in an Eulerian domain as a cuboid with a domain size of 400 mm × 400 mm in X-Y plane and 2000 mm along the tube axis. The model had 100 mm of air along the tube axis behind the plate to ensure that the plate remained in air during deformation caused by shock wave loading. The air inside the tube was also modelled in the Eulerian domain with the element size of 3 mm. All the fluid elements were meshed with the Eulerian eight-node, one-integration point hexahedral elements EC3D8R. The acoustic structural coupling between the fluid-mesh acoustic pressure and the CFRP panel structural displacements was accomplished with a surface-based tie constraint at their common surface. The master-slave type of contact was established between the annular surface of the shock tube in contact with the CFRP panel and the top surface of the panel. The surface of the external fluid at the interface was designated as the master surface. This pairing created an internal coupling of the acoustic pressure and structural displacements at 14 the surface nodes of CFRP panel (slave) and coupled the acoustic pressure exerted through the shock tube to the fluid mesh acoustic pressure at the interface. The incident wavefront was assumed to be planar. For a planar wave, which does not decay, two reference points, namely, the standoff point and the source point, were defined, the relative positions of which were used to determine the travel direction of the incident shock wave. The pressure history at the standoff point was used to drive the incident wave. The 'amplitude' definition was used specifying the top surface of the CFRP panel to which the incident-wave loading was applied using a pressure-history curve.

The entire analysis was divided into two steps pertaining to the wave incidence and reflection, where an appropriate average shock wave velocity and density was used. Linear fluid mechanics was used. The observed total pressure in the fluid was decomposed into two components: the incident wave itself, which was known, and the wave field excited in the fluid due to reflections at the fluid boundaries and interactions with the solid. The setup of the FE model of the shock loading in the CFRP panel with coupled fluid-structure domain is shown in Fig. 1. Panels with three different radii of curvature were utilized in the modelled experiments: infinite (i.e. flat; Panel A), 304.8 mm (Panel B) and 111.8 mm (Panel C).

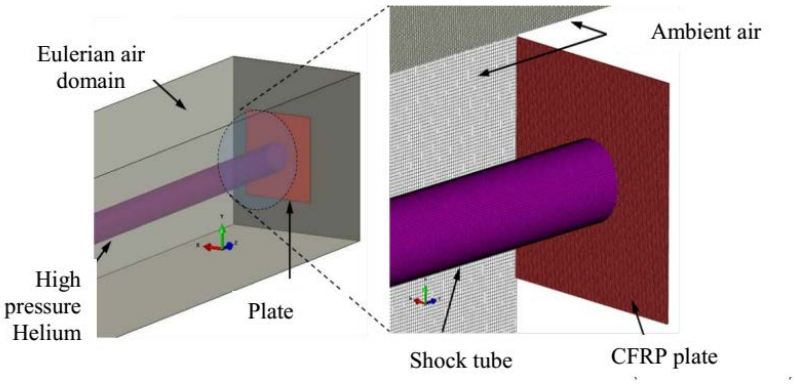

Figure 1. FE model setup for blast simulations

2.6 Modelling details for ballistics in woven composites

A schematic of the developed FE model for ballistics in woven composites is shown in Figure 2. Both woven fabric plate and bullet were modelled as 3D continuum deformable solids. The dynamic explicit solver was used in simulations to account for the time-dependent loading and the complex interaction between the bullet and the fabric composite plate. A 3 mm-thick symmetric cross-ply laminate in this FE model consisted of 12 plies, with an individual ply thickness of 0.25 mm. The local co-ordinate systems were defied to account for orientations of individual plies and to model the laminate and material behaviour precisely. The cylindrical bullet of mass 6.42 g and length 25.3 mm impacts the centre of the workpiece in the axial direction using a velocity boundary condition.

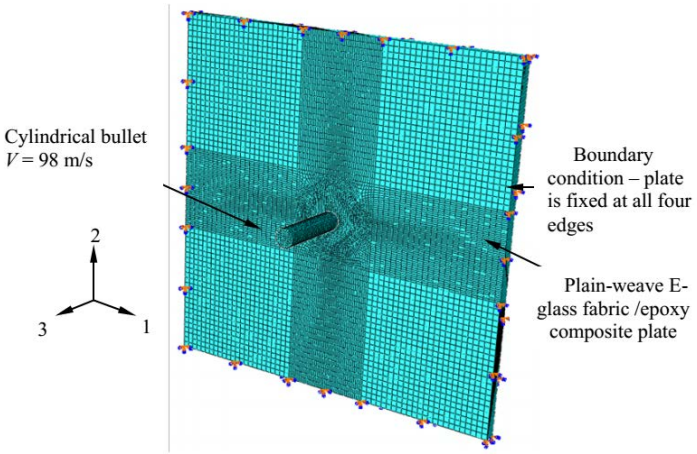

Figure 2. FE model setup for ballistic simulations

3. Results and Discussion

The results of FE models are discussed below. The FE simulations analyse the out-of plane deflection response of FRP plates and their energy absorption capacity under blast and impact loading. Here, only the key findings are discussed.

3.1. Deflections in blast events

The FE analysis demonstrated that deflection of the studied CFRP panels was the combined result of two deflection modes, namely, the indentation mode and the flexure mode. It was found that all the panels started deflecting in the indentation mode initially (Fig. 3). In the flat

panel (Panel A), the global flexural mode quickly began dominating the deflection process. This was confirmed by the continuous nature of displacement contours that show a monotonic increase in deflection from the edge to the centre of the specimen after T = 200 μs. Deflection of Panel B continued in the indentation mode up to about 400 μs, after which it changed to the global flexural deflection mode.

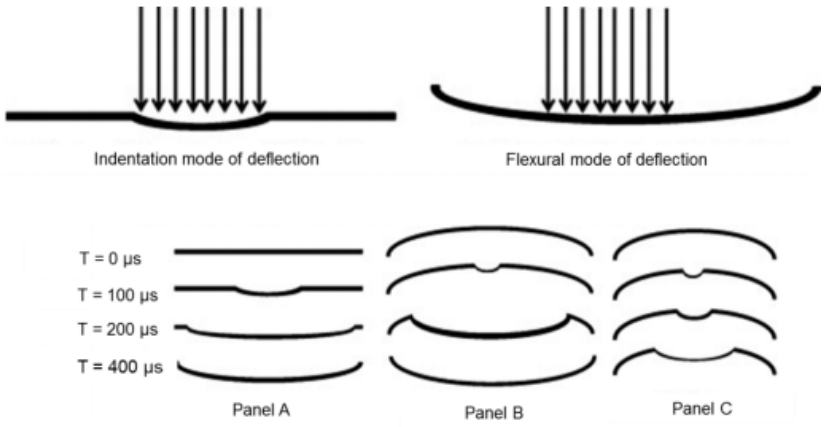

Figure 3. Modes of indentation of CFRP panels (blast pressure for Panel A =4.6 MPa, Panel B = 3.5 MPa and Panel C =7.8 MPa)

These deflection contours show a continuous increase in deflection from the edge to the centre of panel and the transition from elliptical contours back to the circular shape. In Panel C, the deflection was observed to be less than that in Panels A and B since only the central loading region was affected. The in-plain strain output was requested for a set of four elements located at the centre of the back face of panels and its average magnitude was calculated. Figure 4 shows that the deflection rate (35 m/s), for the initial 200 μs, was almost the same for all the three panels, though Panels A and B attained a higher deflection as compared to Panel C. This means that the Panel C was stiffer than the other two panels since it sustained a higher pressure and had a lower deflection. Panels A and B showed similar trends up to 1000 μs. At this time, damage was observed to initiate in Panel B, which explains the rapid increase in its deflection.

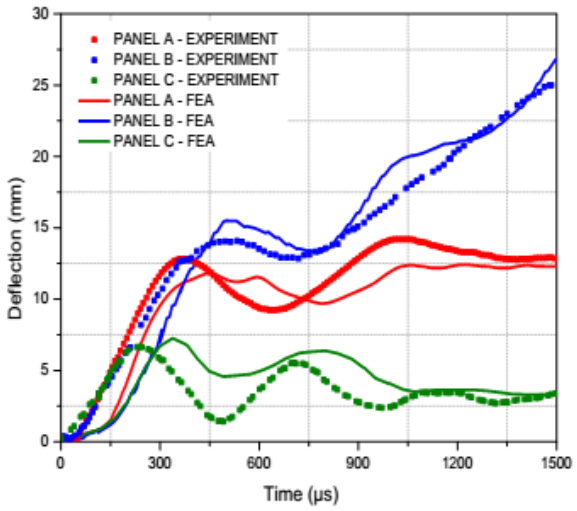

Figure 4. Experimental and numerical results: out-of-plane deflections at the centre of the back face of CFRP panels (blast pressure for Panel A =4.6 MPa, Panel B = 3.5 MPa and Panel C =7.8 MPa)

3.1. Ballistic simulations

The effect of increase in the thickness of composite plate on the ballistic limit velocity (V50) is shown in Figure 5, and the magnitudes of V_{50} are listed in Table 1.

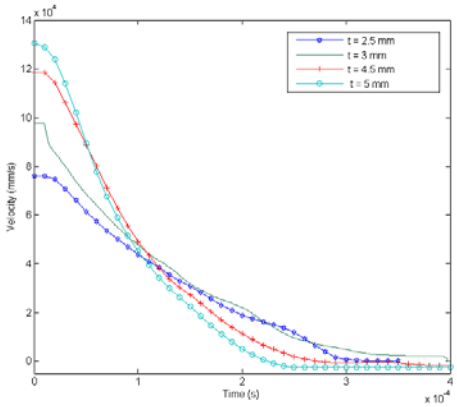

Figure 5. Effect of composite plate thickness on ballistic limit velocity (V_{50})

Thickness of composite plate [mm]	**FE analysis (V_{50})**	**Experiments (V_{50})**
2.5	73.5	72
4.5	118.5	118
5	130.5	130

Table 1. Comparison of ballistic limit velocity

It can be observed form Table 5 that the increase in plate thickness by 66% (considering t = 3 mm as the base plate thickness) resulted in a higher ballistic limit increase by 33%, while decrease in plate thickness by 16% caused reduction in V_{50} by 25%. It was found that the kinetic energy absorbed by the composite plate during impact did not increase linearly with increase in the plate thickness; thus, the primary reason of this increase in the ballistic limit can be attributed to the prolonged contact. It can be safely assumed that at high loading rates, as normally observed in ballistics, the glass fabric undergoes considerable hardening, before failure – thus providing extended resistance.

4. Conclusions

A FE approach was developed capable to model a vast range of impact events, from blasts to ballistic events. A good correlation was obtained with the experimental data emphasising the effectiveness of this model to predict the mechanical response of woven fabric composites under high-velocity impact loading as well as laminated composites in low blast events.

5. References

[1] R. Rajendran and J.M. Lee. Blast loaded plates. *Marine Structures*, 22:99-127, 2009.

[2] A.S. Tekalur, K. Shivakumar, and A. Shukla. Mechanical behaviour and damage evolution in E-Glass vinyl ester and carbon composites subjected to static and blast loads. *Composites Part B: Engineering*, 39:57–65, 2008.

[3] H. Arora, P. A. Hooper and J. P. Dear. Dynamic response of full-scale sandwich composite structure subject to air-blast loading, *Composites: Part A Applied Science and Manufacturing*, 42:1651-1662, 2011.

[4] K. S. Pandya, J. R. Pothnis, G. Ravikumar and N. K. Naik. Ballistic impact behaviour of hybrid composites. *Materials & Design*, 44:128-135, 2013.
[5] G. Zhu, W. Goldsmith and C. K. H. Dharan. Penetration of laminated Kevlar by projectiles: Experimental investigation. *International Journal of Solids and Structures*, 29:399–420, 1992.
[6] R.M. Jones, *Mechanics of composite materials*, Taylor and Francis, 2nd ed., 1999.
[7] *Abaqus 6.13 User Manual.* Dassault System Rhode Island US.
[8] V. A. Phadnis, F. Makhdum, A. Roy and V.V. Silberschmidt. Drilling in carbon/epoxy composites: Experimental investigations and finite element implementation. *Composites Part A - Applied Science and Manufacturing*, 47:41-51, 2013.
[9] Z. Hashin. Analysis of cracked laminates: a variational approach. *Mechanics of Materials*, 4: 121-136, 1985.
[10] A. Puck and H. Schürmann. Failure analysis of FRP laminates by means of physically based phenomenological models. *Composites Science and Technology*, 58:1045-1067, 1998.
[11] P. Maimí, P.P. Camanho, J.A. Mayugo and C.G. Dávila. A thermodynamically consistent damage model for advanced composites. *Technical Report* NASA/TM-214282 Langley US, 2006.
[12] V. S. Sokolinsky, K.C. Indermuehle and J. A. Hurtado, Numerical simulation of the crushing process of a corrugated composite plate. *Composites Part A: Applied Science and Manufacturing.* 42:1119-1126, 2011.